

## SYNTHESIS OF SnO<sub>2</sub>/TiO<sub>2</sub> PHOTOCATALYST FOR REMOVAL OF OXYTETRACYCLINE ANTIBIOTIC IN AQUEOUS SOLUTION

NGUYỄN CHÍ HIẾU<sup>1</sup>, MAI THỂ TÙNG<sup>1</sup>, TRẦN THỊ TƯỜNG VÂN<sup>1\*</sup>

<sup>1</sup>*Institute of Environmental Science, Engineering and Management,  
Industrial University of Ho Chi Minh City*

\* *Corresponding author: tranthituongvan@iuh.edu.vn*

*DOIs: <https://www.doi.org/10.46242/jstiuh.v80i2.5898>*

**Abstract.** In this study, TiO<sub>2</sub>/SnO<sub>2</sub> nanomaterials with the different SnO<sub>2</sub> contents of 1%, 5%, 10%, and 15% were synthesized via a facile one-step sol-gel method. Structural characteristics and surface morphology of these materials were assessed through techniques such as X-ray diffraction (XRD) and Scanning Electron Microscopy (SEM). These materials were then subjected to test photocatalyst activity. The photocatalytic performance of the synthesized materials was evaluated to degrade the oxytetracycline (OTC) antibiotic in aqueous solutions under UVC irradiation. The effect of various operating parameters including reaction time, pH value, initial antibiotic concentration, and photocatalyst content on removal efficiency was also investigated. Remarkably, the SnO<sub>2</sub>/TiO<sub>2</sub> material with a 1% SnO<sub>2</sub> of weight demonstrated the best photocatalytic performance. The OTC removal efficiency was achieved of 98.4% after 120 min UVC irradiation. Furthermore, the reuse ability of the synthesized material was demonstrated with OTC removal efficiency maintained at 95.87% after 5 cycles.

**Keywords.** Antibiotic residue, Binary material, Oxytetracycline, Photocatalyst, Tin dioxide, Titanium dioxide.

### 1 INTRODUCTION

The issue of antibiotic residue pollution has become more and more common, posing significant threats to the environmental life and ecosystems, which demands urgent attention and comprehensive solutions [1]. A globally comprehensive study has revealed alarming findings, indicating that approximately two-thirds of water samples collected across 72 countries contain substantial levels of antibiotic residues. A lot of rivers worldwide are polluted by antibiotic remnants. Notably, renowned water bodies such as the England's Thame River are among those affected, with antibiotic concentrations surpassing acceptable limits. This pollution creates an ideal breeding ground for bacteria to thrive and develop resistance against antibiotics, exacerbating the challenge of combating antibiotic-resistant pathogens. Consequently, the remediation of antibiotic residue in water to the permitted limitations before discharging into the water bodies has become urgent action in recent years [2-4].

In Vietnam, the domestic economy has been witnessing the rapid development of some industries such as livestock farming, pharmaceutical production, medical examination and treatment, and many other industries. Besides their economic benefits, these industries also release significant antibiotics during their operations which can follow wastewater going into receiving sources and cause severe pollution to the environment [5]. In addition, the European Union also warned about antibiotic residues in seafood products in Vietnam in 2016. Likewise, statistics from the Department of Agriculture and Rural Development of Soc Trang province in 2016 revealed that there were 5,000-6,000 types of drugs and chemicals for disease prevention and treatment, aquaculture, and environmental treatment available on the market. Unlike developed countries, antibiotics and other pharmaceuticals in Vietnam can be easily purchased and used [6]. Therefore, it is very difficult for aquaculture farmers to choose quality antibiotics that are allowed to circulate in aquaculture industry. In recent years, Vietnam's revenue from processing and exporting seafood products has been increasing and is one of the industries with the largest revenue, leading to the increasing demand to use antibiotics in the aquaculture process. Many livestock farms use cheap, low-quality antibiotics too much, which can easily affect product quality and cause environmental pollution due to antibiotic residues. Using antibiotics to treat bacterial infections has been increased but has not been processed effectively due to limitations in treatment facilities that can lead to their accumulation and biotransformation in the water resources. Antibiotic residues in discharged wastewater can pollute the environmental water and negatively affect human health. Particularly, some antibiotics such as Chloramphenicol, Quinolone, Fluoroquinolone, and Oxytetracycline have been even discovered in shrimp

and fish, causing people's health. Oxytetracycline (OTC) is a widely available antibiotic with one of the main active mechanisms inhibiting bacterial protein synthesis. OTC belongs to the micro aromatic polyketide family, which is synthesized by a type II polyketide synthase [5].

Therefore, investigations have still been carried out to find effective solutions to more thoroughly address the growing threat of antibiotics in water sources. Recently, to decompose antibiotic residues in the water, various methods have been studied such as advanced oxidation treatment, membrane treatment, microbial decomposition, and adsorption using activated carbon. However, these methods still have many technical limitations. Further research is needed to apply effectively these methods in treating practical wastewater containing antibiotics [7, 8]. Among these methods, photocatalysis has been one of the most potential methods to apply for removing antibiotics from aqueous solution [9]. As well-known that photocatalysis is usually chosen as a green and promising option for the degradation of toxic organic pollutants that harm air and water resources [10, 11]. The advantages of this method include low cost, high photocatalytic performance, chemical stability and environmental friendliness [7, 9, 10].

TiO<sub>2</sub> semiconductor is the most common photocatalyst used in environmental treatment such as air pollution control and decomposition of pollutants in water [11, 12]. However, the application of TiO<sub>2</sub> nanomaterials in real wastewater treatment still has some drawbacks such as high bandgap energy of TiO<sub>2</sub> ( $\geq 3.2\text{eV}$ ), low lifetime of photogenerated electron-hole pairs, and difficulty in separation of finely powdered TiO<sub>2</sub> from treated water for recycling or regenerating it [13]. To overcome these limitations, some modifications to TiO<sub>2</sub> have been used such as coupled with other semiconductors [14-18], fixed in the large surface material (carbon-based material, mesoporous material, zeolite, etc.) [19-22], or doping/co-doping with the metal or non-metallic elements [15, 23-26]. Results of combining two or three semiconductors have demonstrated that the photocatalytic performance of the photocatalyst composite could be improved due to the reduction of band gap and the decrease in electron-hole recombination [17, 27-29].

Among semiconductors used to couple of TiO<sub>2</sub>, tin oxide (SnO<sub>2</sub>) has been considered as one of the most potential metal oxide materials owing the excellent lattice match between TiO<sub>2</sub> and SnO<sub>2</sub>. SnO<sub>2</sub> itself is also known as one of the semiconductor materials with a large bandgap energy ( $\geq 3.6\text{ eV}$ ) [30]. The structure, energy band, and chemical properties of SnO<sub>2</sub> material are similar to TiO<sub>2</sub>, leading to SnO<sub>2</sub> also being used as an effective photocatalytic material [21, 31, 32]. In the field of photocatalysis, SnO<sub>2</sub> nanomaterials and SnO<sub>2</sub>-modified materials have been reported in recent researches to treat pollutants in water [33, 34], such as treating the antibiotic azithromycin with GO/Fe<sub>3</sub>O<sub>4</sub>/ZnO/SnO<sub>2</sub> material [21] and the material combination of g-C<sub>3</sub>N<sub>4</sub>/SnS<sub>2</sub>/SnO<sub>2</sub> used to remove Cr<sup>6+</sup> [35]. However, the investigation on SnO<sub>2</sub>/TiO<sub>2</sub> photocatalytic materials synthesized by sol-gel method to remove antibiotics in aqueous solution is still quite little. Almost of the related researches focused on evaluating the ability to remove dyes and some common organic substances in water [29, 32, 36, 37]. Therefore, in this study we synthesized SnO<sub>2</sub>/TiO<sub>2</sub> photocatalytic materials by a facile one-step sol-gel method. The OTC antibiotic was chosen as a model pollutant to evaluate the photocatalytic performance of the synthesized material. Furthermore, the effect of operation parameters and reusability of materials were also investigated in this work.

## 2 EXPERIMENTAL

### 2.1 Reagents and chemicals

Tetraisopropyl orthotitanate – titan (IV) isopropoxide (TTIP) (C<sub>12</sub>H<sub>28</sub>O<sub>4</sub>Ti, > 99% purity) and propan-2-ol (-C<sub>3</sub>H<sub>8</sub>O, > 99.5% purity) were purchased from Merck Co. Ltd. (Germany). Hexadecyltrimethylammonium bromide (CTAB, >99% purity), tin (IV) chloride pentahydrate (SnCl<sub>4</sub>.5H<sub>2</sub>O, > 98% purity), and oxytetracycline (OTC, C<sub>22</sub>H<sub>24</sub>N<sub>2</sub>O<sub>9</sub>, > 99% purity) were provided by Shanghai Zhanyun Chemical Co. Ltd. (Shanghai, China). Besides, other chemicals such as kali iodide (KI) and 1,4-benzoquinone (C<sub>6</sub>H<sub>4</sub>O<sub>2</sub>), which were used in this work as the scavengers of photocatalysis, were of analytical chemical grade. Water distilled two times was used for all the preparation of chemicals.

### 2.2 Synthesis of SnO<sub>2</sub>/TiO<sub>2</sub> materials

SnO<sub>2</sub>/TiO<sub>2</sub> materials with different mass ratios (0%, 1%, 5%, 10%, and 15%) of SnO<sub>2</sub> were synthesized by the modified sol-gel method with TiO<sub>2</sub> as the base material [38, 39]. In detail, firstly 2.0 g of CTAB was added to 50 mL of ethanol solution. The mixture was continuously stirred for 30 min using a magnetic stirrer. Next, the suitable mass of SnCl<sub>4</sub>.5H<sub>2</sub>O to the desired ratio was added to the mixture under stirring

conditions until SnCl<sub>4</sub>·5H<sub>2</sub>O was completely dissolved. Next, 11.7 mL of TTIP was added to this solution and stirred vigorously for 3 h at room temperature. Then, a few ammonia (25-28%) droplets were dropped gradually into the mixture until a cloudy sol appeared. This mixture was then kept in the ambient air for 24 h for aging purpose. Next, the obtained gel was washed several times with distilled water using a centrifuge (DLAB-DMO636, China). The final solid was dried in an oven (Memmert-UN110, Germany) at 80 °C for 24 h. Finally, the powder was pounded finely with a mortar and calcined in a furnace (Nabertherm-HTC03/15, Germany) at 500 °C for 3 h. The SnO<sub>2</sub>/TiO<sub>2</sub> composites obtained at different mass ratios of SnO<sub>2</sub> 0%, 1%, 5%, 10%, and 15% were denoted as TiSn0, TiSn1, TiSn5, TiSn10, and TiSn15, respectively.

### 2.3 Characterization of the materials

To investigate the crystalline structure of the synthesized materials, the X-ray powder diffraction (XRD) analysis was carried out by an X-ray diffractometer (LabX XRD-6100, Shimadzu, Tokyo, Japan). The patterns were recorded with a scan rate of 2θ/min over the angular (2θ) range of 10-80°. The morphology of the materials was identified using a field-emission scanning electron microscope (FE-SEM, S-4800, Hitachi, Japan).

### 2.4 Photocatalytic experiments

The synthesized materials were evaluated for their photocatalytic ability for the decomposition of OTC solution with a initial concentration of 20 mg/L and at the material content used of 1.0 g/L under UVC light irradiated from a 7-W high-pressure mercury lamp (242 nm, China). Before UVC light illumination, the adsorption was carried out in the dark to obtain adsorption/desorption equilibrium for the material. Then, the photocatalysis was investigated under UVC irradiation for 120 min. At pre-set time intervals, 3 mL of aliquots were taken from the photoreactor and filtered by a 0.45-μm PTFE Nylon syringe filter (Membrane Solutions, Shanghai, China) to remove the material. The concentration of OTC in solution was identified by a UV-visible spectrophotometer (Genesys 105, Thermo Scientific, Madison, WI, US) at wavelength of 360 nm. Moreover, the optimal operating parameters for OTC photodegradation were also carried out using the best material obtained from the previous experiment. In this work, all experiments were repeated three times to achieve high accuracy.

The kinetic equation derived from the Langmuir Hinshelwood model of heterogeneous catalysis is shown in equation (1) [38-40]:

$$\ln\left(\frac{C}{C_0}\right) = -k_T k_a t = -k_{LH} t \quad (1)$$

where  $k_T$ ,  $k_a$ , and  $k_{LH}$  (min<sup>-1</sup>) are specific reaction rate constants for reactant oxidation, reaction equilibrium constant, and the Langmuir–Hinshelwood model rate constant, respectively.  $C_0$  and  $C$  (mg/L) are OTC concentrations at initial and at time ‘t’, respectively.

## 3 RESULTS AND DISCUSSIONS

### 3.1 Characterization of the prepared materials

Figure 1 illustrates the XRD patterns of the synthesized materials. In XRD profile of TiSn0, the typical peaks were observed at diffraction angle 2θ of 25.28°, 38.75°, 48°, 55.7°, 64.02°, 68.96°, 70.34°, and 75.2°, which corresponded to the (101), (004), (200), (211), (204), (116), (220), and (215) planes, respectively. This result confirmed that this synthesis method only formed the TiO<sub>2</sub> anatase phases. In the XRD patterns of TiSn1 and TiSn10, besides the typical peaks of TiO<sub>2</sub> anatase phase, we could observe the presence of the peaks at 27.57° (110), 36.08° (101), 42.18° (111), 56.54° (220), 64.06° (112), which were attributed to the formation of SnO<sub>2</sub> crystallites. In addition, it could be seen that the XRD profiles of TiSn1 and TiSn10 were similar, confirming that the increase in tin content unchanged the phase of the crystallite of TiO<sub>2</sub> and SnO<sub>2</sub>. However, the intensity of the typical peaks of SnO<sub>2</sub> in TiSn10 was stronger than that of TiSn1, implying that the mass of SnO<sub>2</sub> nanoparticles in TiSn10 was larger as compared to TiSn1. These findings demonstrated that TiO<sub>2</sub>/SnO<sub>2</sub> nanocomposites were synthesized successfully by the one-step sol-gel method.

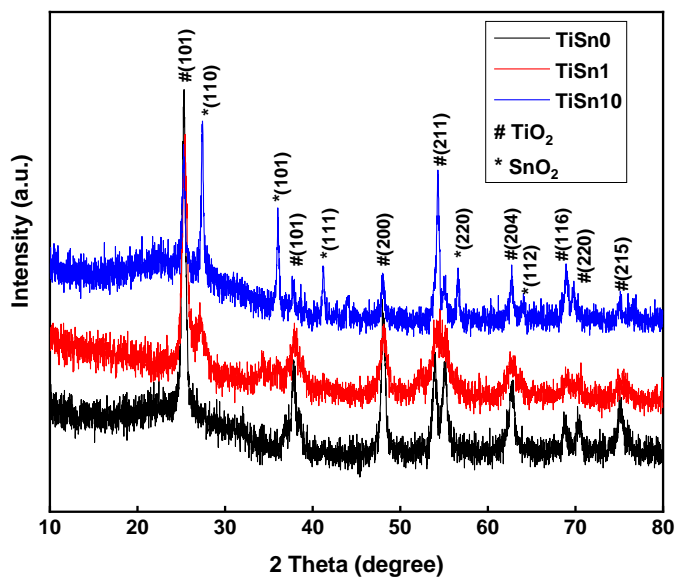


Figure 1: X-ray diffraction spectra of TiSn0, TiSn1 and TiSn10 materials.

The FE-SEM images of the prepared materials are illustrated in figure 2. The FE-SEM image of TiSn0 material (figure 2a) shows the formed TiO<sub>2</sub> nanoparticles with rather uniform shapes, which had a raw spherical structure with particle size in the range of 13-20 nm. In figure 2b, it could be observed that adding SnO<sub>2</sub> with an amount of 1% weight seemed to reduce the average size of the sphere particles of TiSn1 as compared to TiSn0. Furthermore, the shape of TiSn1 nanoparticles was less homogeneous, i.e. with more wider size range than that of TiSn0, implying the presence of SnO<sub>2</sub> in TiO<sub>2</sub>/SnO<sub>2</sub> nanocomposites. This result could be explained by the fact that Sn<sup>4+</sup> added to the synthesis process could affect the formation of the crystal lattice of TiO<sub>2</sub>.

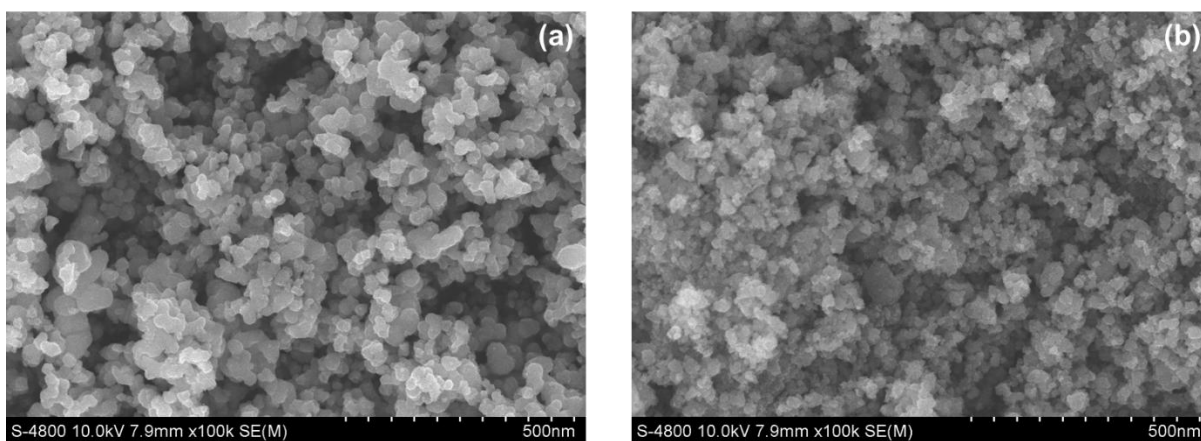


Figure 2: FE-SEM images of pure TiO<sub>2</sub> (a) and TiSn1(b) material.

### 3.2 Photocatalytic performance of the synthesized materials

The results of evaluating OTC photodegradation efficiency using the synthesized materials with the various SnO<sub>2</sub> ratios (figure 3) showed that in general the TiSn1 material demonstrated the highest performance. It could be seen in figure 3a that the adsorptive capacity of all TiO<sub>2</sub>/SnO<sub>2</sub> nanocomposites after 30 stirring minutes in the dark was higher than that of TiSn0 (only pure TiO<sub>2</sub>). In detail, the OTC removal efficiency by adsorption using TiSn0 only obtained 17.4%. Meanwhile, these values when using TiSn1, TiSn5, TiSn10, and TiSn15 rose gradually from 21.9% to 29.7%. This result indicated that the introduction of SnO<sub>2</sub> might change the surface area of TiO<sub>2</sub>/SnO<sub>2</sub> nanocomposites as compared to pure TiO<sub>2</sub>, which improved their OTC adsorptive ability. Figures. 3a, b and c show the changing of OTC removal efficiency,

OTC concentration and kinetic of the OTC photocatalytic degradation using the different materials during 120 min irradiation with UVC light. The highest OTC degradation efficiency (98.4%) was achieved for TiSn1. With the larger SnO<sub>2</sub> ratios (5%, 10%, and 15%) in TiO<sub>2</sub>/SnO<sub>2</sub> nanocomposites, the OTC removal efficiency using these materials was decreased, even lower than that of TiSn0. From calculation on the kinetics of OTC photodegradation (figure 3c), the highest apparent constant rate ( $k_{app}$ ) of OTC photodegradation was obtained for TiSn1 (0.44 min<sup>-1</sup>), followed by in order TiSn0 (0.27 min<sup>-1</sup>) > TiSn10 (0.23 min<sup>-1</sup>) > TiSn5 (0.20 min<sup>-1</sup>) > TiSn15 (0.17 min<sup>-1</sup>). Although photocatalytic activity of SnO<sub>2</sub> nanoparticles could be lower than TiO<sub>2</sub> nanoparticles, the addition of suitable tin content during synthesis could enhance the photocatalytic activity of the TiO<sub>2</sub>/SnO<sub>2</sub> nanocomposites. This result could be explained by (i) the formation defect in the TiO<sub>2</sub> crystallite due to the presence of Sn<sup>4+</sup> ions and (ii) the formation of SnO<sub>2</sub> nanoparticles attached on the surface of TiO<sub>2</sub> nanoparticles when the suitable SnCl<sub>4</sub> mass was added during synthesis, which could improve the lifetime of electron-hole pairs formed in photocatalysis [29].

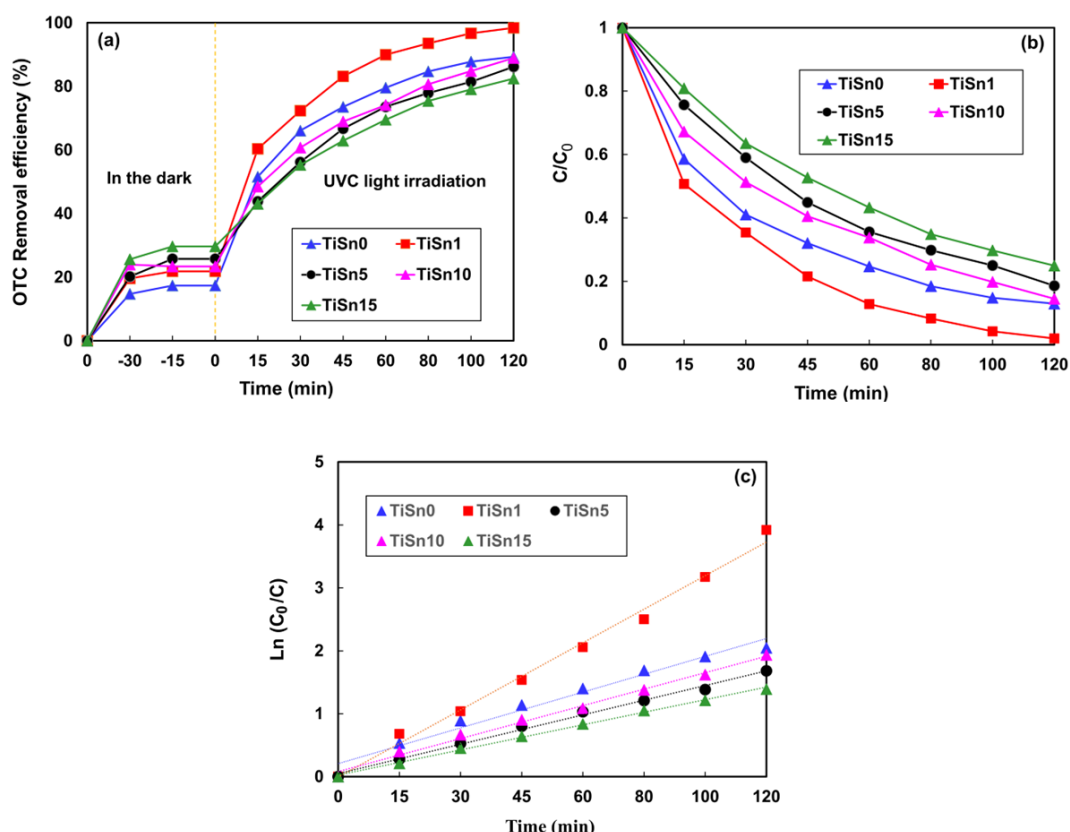


Figure 3: (a) OTC removal efficiency by adsorption and photocatalysis, (b) changing of  $C/C_0$  value under UVC irradiation, (c) kinetic of OTC photocatalytic degradation with the different materials.

To evaluate the effect of initial OTC concentration on removal efficiency for the TiSn1 material, the different OTC concentrations were investigated at 10 mg/L, 20 mg/L, 45 mg/L, and 60 mg/L. Figure 4 reveals the photocatalytic performance using TiSn1 at the different OTC concentrations. Obviously, an increase in the initial OTC concentration led a decrease in the OTC removal efficiency. In detail, the OTC removal efficiency achieved 99.2% and 98.4% at two concentrations of 10 mg/L and 20 mg/L, respectively. At the high initial OTC concentrations of 45 mg/L and 60 mg/L, the removal efficiency decreased significantly to more than 60%. This could be explained by the fact that too many antibiotic molecules could adhere to and cover the photocatalysts' surface, hindering the process of light rays reaching the surface of the TiSn1 material and reducing the formation of the oxidation species such as hydroxyl radicals ( $\bullet\text{OH}$ ), superoxide ( $\bullet\text{O}_2^-$ ), etc. Another reason could be that the activated groups generated from the photocatalytic process were insufficient to react to the OTC molecules present in the solution, leading to a decrease in photocatalytic performance at the high OTC concentrations.

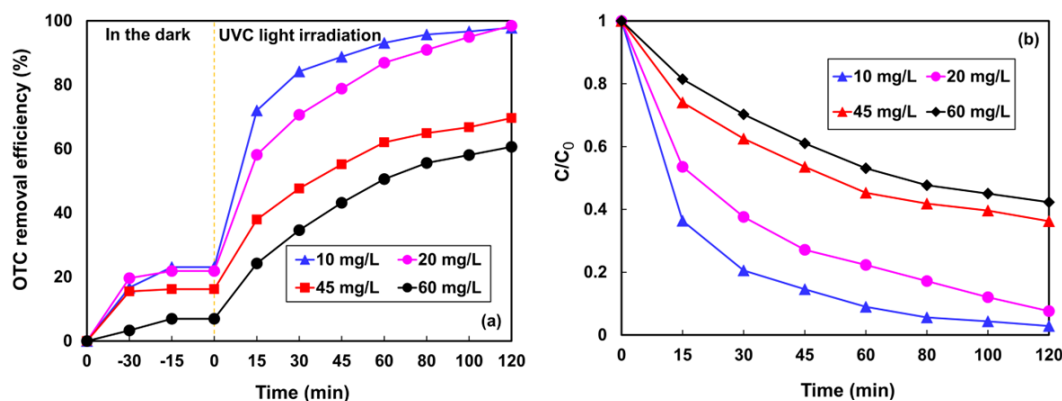


Figure 4: The change in photocatalytic performance using TiSn1 material at the different initial OTC concentrations in aqueous solution (experimental conditions: irradiation by 5 W UVC lamp, material content of 1.0 g/L,  $pH_{\text{nature}}$  7.3, and room temperature).

The concentration of TiSn1 material was changed at 0.5 g/L, 1.0 g/L, and 1.5 g/L to determine the optimal amount of material for OTC antibiotics photodegradation. As seen from figure 5, the highest OTC removal efficiency was achieved at the material concentration of 1.0 g/L (98.4%), followed by 1.5 g/L (94.3 %) and 0.5 g/L (83.9 %). However, the difference in the photocatalytic performance of the TiSn1 material was considered insignificant. Consequently, in this experiment the optimal material content of TiSn1 was obtained at 1.0 g/L, at which the material concentration was selected for the next experiments.

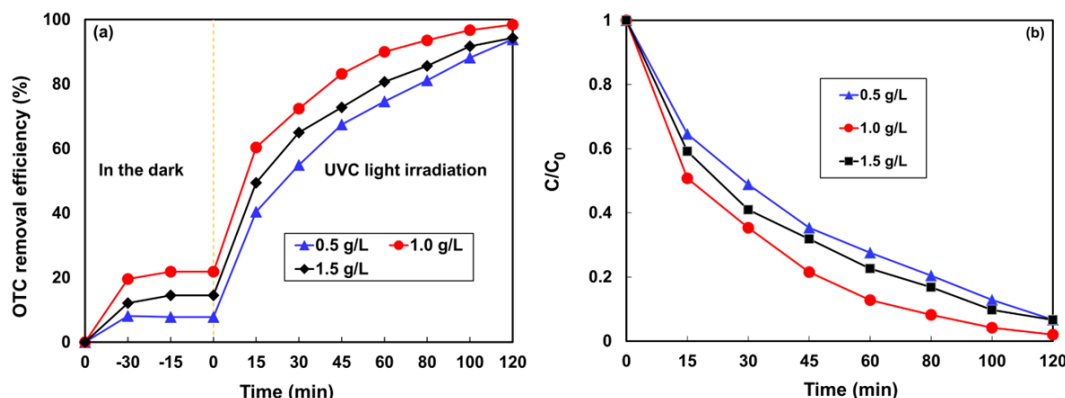


Figure 5: The OTC removal performance of TiSn1 at the various contents of TiSn1 material (experimental conditions: irradiation by 5 W UVC lamp, initial OTC concentration of 20 mg/L, at  $pH_{\text{nature}}$  7.3, and room temperature).

The pH is an important parameter in photocatalytic reactions as it influences forming the active species ( $h^+$ ,  $\bullet OH$  radical, and  $\bullet O_2^-$ ). Besides, the pH value of the solution significantly affects photocatalytic activity, including the charge on the material and the formation of various OTC structures. To investigate the effect of pH values on OTC antibiotics photodegradation using the TiSn1 material, the pH value of OTC solution with an initial concentration of 20 mg/L was changed with pH values of 3, 5, 7, 9, and 11 by adding 0.1 mol/L NaOH or 0.1 mol/L HCl. Figure 6 shows the OTC removal efficiency of the TiSn1 material at the different pH values of 3, 5, 9, and 11. It could be seen clearly that the OTC removal efficiency achieved the highest at an acidic medium (94.3-98.7%). In contrast, the removal efficiency decreased dramatically in the alkaline media with 75.7 % and 66.3 % at pH 9 and 11, respectively.

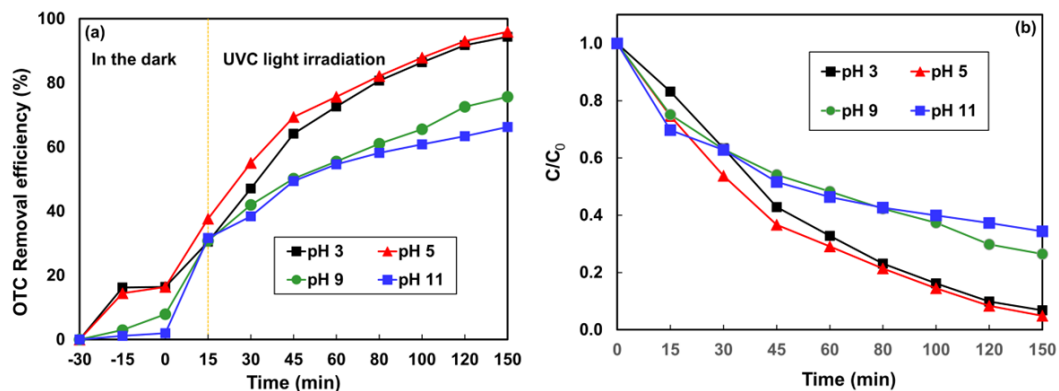


Figure 6: The change in photocatalytic performance using TiSn1 material at the different pH values of aqueous solution (experimental conditions: irradiation by 5 W UVC lamp, initial OTC concentration of 20 mg/L, material content of 1.0 g/L, and room temperature).

To investigate the role of the active species generated by photocatalysis such as holes ( $h^+$ ), superoxide ( $\bullet O_2^-$ ), and hydroxyl radicals ( $\bullet OH$ ) in OTC decomposition reactions using the TiSn1 material, radicals scavenger test was conducted in this work. In this experiment, isopropanol (IPA, a  $\bullet OH$  radical scavenger), potassium iodide (KI, a  $h^+$  hole scavenger), and *p*-benzoquinone (*p*-BQ, a  $\bullet O_2^-$  radical scavenger) solution was added to the 20 mg/L OTC aqueous solution to evaluate effect of active species on the OTC photodegradation using TiSn1. As shown in figure 7, the presence of IPA and KI during photocatalysis decreased the OTC removal efficiency from 98.4 % (no scavenger) to 74.81% ( $\bullet OH$  radical scavenger) and 62.9% ( $h^+$  hole scavenger) after 120 min UVC irradiation. Particularly, the addition of *p*-BQ ( $\bullet O_2^-$  radical scavenger) decreased dramatically the OTC photodegradation, the removal efficiency in this case was only 18.4 % after 120 min UVC irradiation. These results confirmed the important role of  $\bullet O_2^-$ ,  $h^+$ , and  $\bullet OH$  radicals in the photocatalytic degradation reaction of OTC antibiotic in the water of the TiSn1 material. Furthermore, it also demonstrated that  $\bullet O_2^-$  radicals were the major reactive agents in OTC photodegradation. These findings were consistent with our previous research [41].

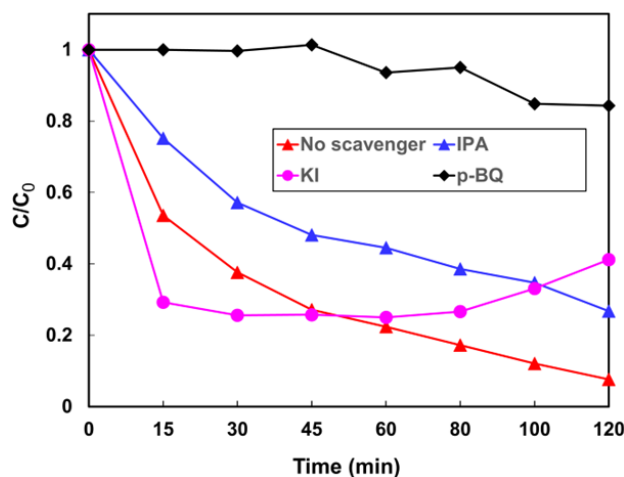


Figure 7: Performance of photocatalytic degradation of OTC antibiotic using TiSn1 material in the presence of scavengers (experimental conditions: initial OTC concentration of 20 mg/L, material content of 1.0 g/L, at  $pH_{\text{nature}}$  7.3, and room temperature).

To test the reusability of the TiSn1 material, a recycle experiment was carried out for 5 cycles. After each cycle, the used material was collected by the sedimentation, centrifugation, and drying process, respectively. The material collected would be used for the next cycle. The experiment results showed that the adsorptive ability of the material decreased in the next cycles (from 25.5% to 10.6%) which could be explained because the material had not been completely removed from OTC molecules adhered to the surface by the regeneration method mentioned above. However, the OTC removal efficiency changed

insignificantly in the following cycles as compared to the first cycle under UVC irradiation. As shown in figure 8, the OTC removal efficiency was maintained over 95% after five cycles. The slight decrease in removal efficiency could be attributed to a certain loss of materials after each regeneration cycle and the reduction of adsorption ability as the main reason. This result demonstrated the good reusability of TiSn1; however, continued research is still needed in order to improve the recovery method of TiSn1 more effective and simpler to expand its practical application.

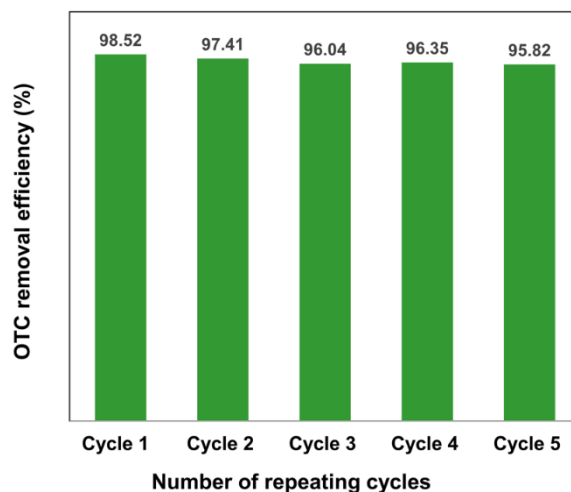


Figure 8: Reusability of the TiSn1 photocatalyst for 5 repeated cycles (experimental conditions: initial OTC concentration of 20 mg/L, at  $\text{pH}_{\text{nature}}$  7.3, and room temperature).

#### 4 CONCLUSIONS

In this study, the  $\text{SnO}_2/\text{TiO}_2$  nanocomposite materials were synthesized successfully using a one-step sol-gel method employing CTAB as a substrate and  $\text{TiO}_2$  as a foundational material. XRD and FE-SEM results confirmed the formation of  $\text{TiO}_2$  and  $\text{SnO}_2$  nanoparticles in the synthesized materials. All the materials presented good photocatalytic activity for OTC removal. The highest photocatalytic performance was achieved at 1% wt. of the  $\text{SnO}_2$  mass ratio, where 98.5 % of OTC removal was obtained after 120 min UVC irradiation using TiSn1. The effect of operating parameters such as antibiotic concentration, material content, and pH value in the solution was also carried out. The experimental results showed that the most efficient OTC removal happened in the acidic medium at a material concentration of 1.0 g/L. The  $\bullet\text{OH}$  radicals were the most important agents in OTC photodegradation using TiSn1. The photocatalytic activity of TiSn1 also maintained more than 95% after five cycles, which implied that TiSn1 could be a promising photocatalyst for the application to remove antibiotics in aqueous solution.

#### ACKNOWLEDGMENT

The authors thank the Institute of Environmental Science, Engineering, and Management (IESEM), Industrial University of Ho Chi Minh City (IUH), Ho Chi Minh City, Vietnam for the support on experimental apparatus used in this research.

#### REFERENCES

- [1] X. Qu, P. J. J. Alvarez, and Q. Li, Applications of nanotechnology in water and wastewater treatment, *Water Research*, vol. 47, no. 12, pp. 3931-3946, 2013.
- [2] T. C. M. V. Do, D. Q. Nguyen, K. T. Nguyen, and P. H. Le,  $\text{TiO}_2$  and Au- $\text{TiO}_2$  Nanomaterials for Rapid Photocatalytic Degradation of Antibiotic Residues in Aquaculture Wastewater, *Materials*, vol. 12, no. 15, p. 2434, 2019.
- [3] A. N. Ngigi, M. M. Magu, and B. M. Muendo, Occurrence of antibiotics residues in hospital wastewater, wastewater treatment plant, and in surface water in Nairobi County, Kenya, *Environmental monitoring and assessment*, vol. 192, no. 1, p. 18, 2020.

- [4] Q. Wang, P. Wang, and Q. Yang, Occurrence and diversity of antibiotic resistance in untreated hospital wastewater, *Science of The Total Environment*, vol. 621, pp. 990-999, 2018.
- [5] Z. Wang, X. Wang, H. Tian, Q. Wei, B. Liu, G. Bao, M. Liao, J. Peng, X. Huang, and L. Wang, High through-put determination of 28 veterinary antibiotic residues in swine wastewater by one-step dispersive solid phase extraction sample cleanup coupled with ultra-performance liquid chromatography-tandem mass spectrometry, *Chemosphere*, vol. 230, pp. 337-346, 2019.
- [6] C. Stålsby Lundborg and A. Tamhankar, Antibiotic residues in the environment of South East Asia, *BMJ*, vol. 358, p. j2440, 2017.
- [7] X. Yang, Z. Chen, W. Zhao, C. Liu, X. Qian, M. Zhang, G. Wei, E. Khan, Y. H. Ng, and Y. S. Ok, Recent advances in photodegradation of antibiotic residues in water, *Chemical Engineering Journal*, vol. 405, p. 126806, 2021.
- [8] B. Bethi, S. H. Sonawane, B. A. Bhanvase, and S. P. Gumfekar, Nanomaterials-based advanced oxidation processes for wastewater treatment: A review, *Chemical Engineering and Processing - Process Intensification*, vol. 109, pp. 178-189, 2016.
- [9] N. Roy, S. A. Alex, N. Chandrasekaran, A. Mukherjee, and K. Kannabiran, A comprehensive update on antibiotics as an emerging water pollutant and their removal using nano-structured photocatalysts, *Journal of Environmental Chemical Engineering*, vol. 9, no. 2, p. 104796, 2021.
- [10] D. Zhu and Q. Zhou, Action and mechanism of semiconductor photocatalysis on degradation of organic pollutants in water treatment: A review, *Environmental Nanotechnology, Monitoring & Management*, vol. 12, p. 100255, 2019.
- [11] R. Ata and G. Y. Töre, Characterization and removal of antibiotic residues by NFC-doped photocatalytic oxidation from domestic and industrial secondary treated wastewaters in Meric-Ergene Basin and reuse assessment for irrigation, *Journal of environmental management*, vol. 233, pp. 673-680, 2019.
- [12] B. Pant, M. Park, and S.-J. Park, Recent advances in TiO<sub>2</sub> films prepared by sol-gel methods for photocatalytic degradation of organic pollutants and antibacterial activities, *Coatings*, vol. 9, no. 10, p. 613, 2019.
- [13] A. R. Khataee, M. Zarei, M. Fathinia, and M. K. Jafari, Photocatalytic degradation of an anthraquinone dye on immobilized TiO<sub>2</sub> nanoparticles in a rectangular reactor: Destruction pathway and response surface approach, *Desalination*, vol. 268, no. 1-3, pp. 126-133, 2011.
- [14] N. Moghni, H. Boutoumi, H. Khalaf, N. Makaoui, and G. Colón, Enhanced photocatalytic activity of TiO<sub>2</sub>/WO<sub>3</sub> nanocomposite from sonochemical-microwave assisted synthesis for the photodegradation of ciprofloxacin and oxytetracycline antibiotics under UV and sunlight, *Journal of Photochemistry and Photobiology A: Chemistry*, vol. 428, p. 113848, 2022.
- [15] I. Ibrahim, G. V. Belessiotis, M. Antoniadou, A. Kaltzoglou, E. Sakellis, F. Katsaros, L. Sygellou, M. K. Arfanis, T. M. Salama, and P. Falaras, Silver decorated TiO<sub>2</sub>/g-C<sub>3</sub>N<sub>4</sub> bifunctional nanocomposites for photocatalytic elimination of water pollutants under UV and artificial solar light, *Results in Engineering*, vol. 14, p. 100470, 2022.
- [16] H. P. Nguyen, T. M. Cao, T.-T. Nguyen, and V. V. Pham, Improving photocatalytic oxidation of semiconductor (TiO<sub>2</sub>, SnO<sub>2</sub>, ZnO)/CNTs for NO<sub>x</sub> removal, *Journal of Industrial and Engineering Chemistry*, vol. 127, pp. 321-330, 2023.
- [17] M. L. A. Kumari, L. G. Devi, G. Maia, T.-W. Chen, N. Al-Zaqri, and M. A. Ali, Mechanochemical synthesis of ternary heterojunctions TiO<sub>2</sub>(A)/TiO<sub>2</sub>(R)/ZnO and TiO<sub>2</sub>(A)/TiO<sub>2</sub>(R)/SnO<sub>2</sub> for effective charge separation in semiconductor photocatalysis: A comparative study, *Environmental Research*, vol. 203, p. 111841, 2022.
- [18] C. H. Nguyen, M. L. Tran, T. T. V. Tran, and R.-S. Juang, Enhanced removal of various dyes from aqueous solutions by UV and simulated solar photocatalysis over TiO<sub>2</sub>/ZnO/rGO composites, *Separation and Purification Technology*, vol. 232, p. 115962, 2020.
- [19] Z. Zhao, X. Ma, Q. Xie, Y. Ye, Q. Wang, and H. Zhang, Adsorptive-photocatalytic removal of oxytetracycline by mesoporous silicates immobilized N-doped TiO<sub>2</sub> nanoparticles: A comparative study on effect of support, *Optical Materials*, vol. 131, p. 112666, 2022.
- [20] C. Shaniba, M. Akbar, K. Ramseena, P. Raveendran, B. N. Narayanan, and R. M. Ramakrishnan, Sunlight-assisted oxidative degradation of cefixime antibiotic from aqueous medium using TiO<sub>2</sub>/nitrogen doped holey graphene nanocomposite as a high performance photocatalyst, *Journal of Environmental Chemical Engineering*, vol. 8, no. 1, p. 102204, 2020.
- [21] M. H. Sayadi, S. Sobhani, and H. Shekari, Photocatalytic degradation of azithromycin using GO@Fe<sub>3</sub>O<sub>4</sub>/ZnO/SnO<sub>2</sub> nanocomposites, *Journal of cleaner production*, vol. 232, pp. 127-136, 2019.
- [22] X. Zhang, Y. Xia, L. Zhang, Y. Luo, L. Xu, Q. Zhou, Q. Yu, X. Zhu, and W. Feng, Effects of SnO<sub>2</sub> coupling on the structure and photocatalytic performance of TiO<sub>2</sub>/sepiolite composites, *Journal of Saudi Chemical Society*, vol. 27, no. 6, p. 101765, 2023.
- [23] O. Nasr, O. Mohamed, A.-S. Al-Shirbini, and A.-M. Abdel-Wahab, Photocatalytic degradation of acetaminophen over Ag, Au and Pt loaded TiO<sub>2</sub> using solar light, *Journal of Photochemistry and Photobiology A: Chemistry*, vol. 374, pp. 185-193, 2019.

- [24] S. Zamani, M. R. Rahimi, and M. Ghaedi, Spinning disc photoreactor based visible-light-driven Ag/Ag<sub>2</sub>O/TiO<sub>2</sub> heterojunction photocatalyst film toward the degradation of amoxicillin, *Journal of Environmental Management*, vol. 303, p. 114216, 2022.
- [25] T. Suwannaruang, J. P. Hildebrand, D. H. Taffa, M. Wark, K. Kamonsuangkasem, P. Chirawatkul, and K. Wantala, Visible light-induced degradation of antibiotic ciprofloxacin over Fe–N–TiO<sub>2</sub> mesoporous photocatalyst with anatase/rutile/brookite nanocrystal mixture, *Journal of Photochemistry and Photobiology A: Chemistry*, vol. 391, p. 112371, 2020.
- [26] K. Wannakan, K. Khansamrit, T. Senasu, T. Chankhanittha, and S. J. A. Nanan, Ag-Modified ZnO for Degradation of Oxytetracycline Antibiotic and Reactive Red Azo Dye, *Antibiotics*, vol. 11, no. 11, p. 1590, 2022.
- [27] J. Paniagua-Méndez, S. L. Ramírez-Sandoval, E. Reyes-Uribe, and M. E. Contreras-García, Photocatalytic activity and biocide effect of nanostructured SnO<sub>2</sub>/ZnO/TiO<sub>2</sub> thin film heterostructure obtained by sol-gel spin coating technique, *Ceramics International*, 2024.
- [28] Y. Li, X. Zhang, X. Hu, Z. Li, J. Fan, and E. Liu, Facile fabrication of SnO<sub>2</sub>/TiO<sub>2</sub> nanotube arrays for efficient degradation of pollutants, *Optical Materials*, vol. 127, p. 112252, 2022.
- [29] R. B. Rajput, S. N. Jamble, and R. B. Kale, A review on TiO<sub>2</sub>/SnO<sub>2</sub> heterostructures as a photocatalyst for the degradation of dyes and organic pollutants, *Journal of Environmental Management*, vol. 307, p. 114533, 2022.
- [30] C. M. Magdalane, K. Kanimozhi, M. V. Arularasu, G. Ramalingam, and K. Kaviyarasu, Self-cleaning mechanism of synthesized SnO<sub>2</sub>/TiO<sub>2</sub> nanostructure for photocatalytic activity application for waste water treatment, *Surfaces and Interfaces*, vol. 17, p. 100346, 2019.
- [31] V. K. Gupta, R. Saravanan, S. Agarwal, F. Gracia, M. M. Khan, J. Qin, and R. V. Mangalaraja, Degradation of azo dyes under different wavelengths of UV light with chitosan-SnO<sub>2</sub> nanocomposites, *Journal of Molecular Liquids*, vol. 232, pp. 423-430, 2017.
- [32] S. P. Kim, M. Y. Choi, and H. C. Choi, Photocatalytic activity of SnO<sub>2</sub> nanoparticles in methylene blue degradation, *Materials Research Bulletin*, vol. 74, pp. 85-89, 2016.
- [33] H. Xiao, F. Qu, A. Umar, and X. Wu, Facile synthesis of SnO<sub>2</sub> hollow microspheres composed of nanoparticles and their remarkable photocatalytic performance, *Materials Research Bulletin*, vol. 74, pp. 284-290, 2016.
- [34] W. Sangchay, The Self-cleaning and Photocatalytic Properties of TiO<sub>2</sub> Doped with SnO<sub>2</sub> Thin Films Preparation by Sol-gel Method, *Energy Procedia*, vol. 89, pp. 170-176, 2016.
- [35] Y. Yang, X.-A. Yang, D. Leng, S.-B. Wang, and W.-B. Zhang, Fabrication of g-C<sub>3</sub>N<sub>4</sub>/SnS<sub>2</sub>/SnO<sub>2</sub> nanocomposites for promoting photocatalytic reduction of aqueous Cr(VI) under visible light, *Chemical Engineering Journal*, vol. 335, pp. 491-500, 2018.
- [36] P. C. Hernández-Del Castillo, J. Oliva, and V. Rodriguez-Gonzalez, An eco-friendly and sustainable support of agave-fibers functionalized with graphene/TiO<sub>2</sub>:SnO<sub>2</sub> for the photocatalytic degradation of the 2,4-D herbicide from the drinking water, *Journal of Environmental Management*, vol. 317, p. 115514, 2022.
- [37] V. Bagga, N. Singh, M. Khanuja, M. Rani, and D. Kaur, Enhanced photocatalytic degradation of Rhodamine B and Methylene blue by novel TiO<sub>2</sub>/SnSe-SnO<sub>2</sub> hybrid nanocomposites under sunlight irradiation: Correlation of photoluminescence property with photocatalytic activity, *Materials Research Bulletin*, vol. 159, p. 112109, 2023.
- [38] S. Hassan, A. Ahmed, and M. Mannaa, Preparation and characterization of SnO<sub>2</sub> doped TiO<sub>2</sub> nanoparticles: Effect of phase changes on the photocatalytic and catalytic activity, *Journal of Science: Advanced Materials and Devices*, vol. 4, 2019.
- [39] S. M. Hassan, A. I. Ahmed, and M. A. Mannaa, Structural, photocatalytic, biological and catalytic properties of SnO<sub>2</sub>/TiO<sub>2</sub> nanoparticles, *Ceramics International*, vol. 44, no. 6, pp. 6201-6211, 2018.
- [40] Y. Liu, X. He, Y. Fu, and D. D. Dionysiou, Degradation kinetics and mechanism of oxytetracycline by hydroxyl radical-based advanced oxidation processes, *Chemical Engineering Journal*, vol. 284, pp. 1317-1327, 2016.
- [41] C. H. Nguyen, T. T. V. Tran, M. L. Tran, and R.-S. Juang, Facile synthesis of reusable Ag/TiO<sub>2</sub> composites for efficient removal of antibiotic oxytetracycline under UV and solar light irradiation, *Journal of the Taiwan Institute of Chemical Engineers*, vol. 145, p. 104825, 2023.

**TỔNG HỢP VẬT LIỆU QUANG XÚC TÁC SnO<sub>2</sub>/TiO<sub>2</sub>  
ỨNG DỤNG XỬ LÝ KHÁNG SINH OXYTETRACYCLINE TRONG NƯỚC**

NGUYỄN CHÍ HIẾU<sup>1</sup>, MAI THỂ TÙNG<sup>1</sup>, TRẦN THỊ TƯỜNG VÂN<sup>1\*</sup>

<sup>1</sup> Viện Khoa học Công nghệ và Quản lý Môi Trường, Trường Đại học Công Nghiệp TP.HCM

\* Tác giả liên hệ: tranthituongvan@iuh.edu.vn

**Tóm tắt.** Trong nghiên cứu này, vật liệu nano TiO<sub>2</sub>/SnO<sub>2</sub> với tỉ lệ 1%, 5%, 10%, và 15% khối lượng của SnO<sub>2</sub> được tổng hợp bằng phương pháp sol-gel đơn giản một bước. Đặc điểm về cấu trúc và hình thái của vật liệu đã được xác định thông qua nhiễu xạ tia X (XRD) và kính hiển vi điện tử quét (SEM). Các vật liệu này sau đó được đánh giá hoạt động quang xúc tác. Hiệu suất quang xúc tác của các vật liệu tổng hợp đã được đánh giá để phân hủy kháng sinh oxytetracycline (OTC) trong dung dịch nước dưới sự chiếu xạ tia UVC. Ảnh hưởng của các thông số vận hành khác nhau bao gồm thời gian phản ứng, giá trị pH, nồng độ kháng sinh ban đầu và nồng độ vật liệu quang xúc tác đối với hiệu quả loại bỏ cũng đã được nghiên cứu. Đáng chú ý, vật liệu SnO<sub>2</sub>/TiO<sub>2</sub> với 1% SnO<sub>2</sub> về trọng lượng (TiSn1) đã thể hiện hiệu suất quang xúc tác tốt nhất. Hiệu suất loại bỏ OTC đạt được là 98,7% sau 120 phút chiếu xạ UVC. Hơn nữa, khả năng tái sử dụng của vật liệu tổng hợp cũng đã được chứng minh với hiệu quả loại bỏ OTC duy trì ở mức 95,87% sau 5 lần tái sử dụng.

**Từ khóa.** Dư lượng kháng sinh, Vật liệu nhị phân, Oxytetracycline, Chất xúc tác quang, Oxit thiếc, Dioxit titan.

*Received on July 01 – 2024*

*Revised on December 16 – 2025*